Article

MODELLING UNCERTAINTY CAUSED BY INTERNAL WAVES ON THE ACCURACY OF MBES

By Travis HAMILTON[1] and Jonathan BEAUDOIN[2] (CANADA)
(1) Ocean Mapping Group, University of New Brunswick
(2) Centre for Coastal and Ocean Mapping, University of New Hampshire

Abstract

A 3D ray tracing model has been developed to estimate the effects of internal waves upon the accuracy of multibeam echosounders (MBES). A case study examines the variability in these effects as a function of survey line direction and also considers the case of improving 2D ray tracing models with wave parameters derived from MBES water column imagery. Results indicate that, under certain circumstances, the effects of internal waves can prove to be a significant source of uncertainty that detracts from the ability to efficiently map the seafloor with wide swath angles.

Résumé

Un modèle de traçage à rayons tridimensionnels a été développé en vue d'évaluer les effets des ondes internes sur l'exactitude des échosondeurs multifaisceaux (MBES). Une étude de cas examine la variabilité sur ces effets comme fonction de la direction des lignes de sondes et traite également de l'amélioration des modèles de traçage à rayons bidimensionnels avec des paramètres d'ondes tirés de l'imagerie MBES des colonnes d'eau. Les résultats indiquent que, dans certaines circonstances, les effets des ondes internes peuvent s'avérer une importante source d'incertitudes qui porte atteinte à la capacité de cartographier de manière efficace le fond marin avec de larges angles de couverture.

Resumen

Se ha desarrollado un modelo de seguimiento de rayos en 3D para estimar los efectos de las olas internas en la exactitud de los sondadores acústicos multihaz (MBES). El estudio de un caso examina la variabilidad en estos efectos como función de la dirección de las líneas de sondas y considera también el caso consistente en mejorar el seguimiento de rayos en 2D con parámetros de olas derivados del tratamiento de imágenes de la columna de agua con MBES. Los resultados indican que, en algunas circunstancias, los efectos de las olas internas pueden resultar ser una fuente significativa de incertidumbre que le resta valor a la capacidad de representar eficazmente el fondo del mar con ángulos de corte anchos.

1. Introduction

One of the main sources of uncertainty for MBES soundings comes from refraction of the acoustic ray path due to variations in sound speed in the water column. Since most of the variability in sound speed occurs in the vertical direction, a vertical profile of the sound speed can be used to correct for refraction effects. If an incorrect or outdated sound speed profile is used then the acoustic ray travels along a different path than what was assumed, resulting in vertical and horizontal biases in the final 3D position of the sounding. The ray path is calculated with a ray tracing algorithm. Although there are different algorithms the key to refraction remains in Snell's Law (equation (1)):

$$\frac{\sin\theta 1}{sound\ speed\ 1} = \frac{\sin\theta 2}{sound\ speed\ 2} \qquad (1)$$

where θ_1 is the angle of incidence between the ray and the interface through which it is refracting, and θ_2 is the refracted angle. For ray tracing the interface is between two layers of sound speed (*Sound speed 1* and *Sound speed 2*).

Given that the ocean environment is often generalized as being horizontally stratified, the assumption that sound speed only depends on depth is used for ray tracing (Lurton 2002). This approach greatly simplifies the mathematics in ray tracing models, as well as water column sampling, because it is difficult to measure any deviation from horizontal stratification. This base assumption allows each of the discretely measured layers of speed from a sound speed profile (SSP) to be modeled as a horizontally stratified plane of constant sound speed. With the horizontal stratification assumption, the angle of incidence between a ray and an interface, between two layers of sound speed, will always be relative to the vertical; however, in reality, this is not always the case.

In many areas internal waves occur along the pycnocline ("a layer where density changes most rapidly with depth. It can be associated with either a halocline or a thermocline." (Baum 2004)). This density gradient is often associated with a strong gradient in sound speed (velocline) which acts as a strong refracting layer. Internal waves can introduce a bias into the soundings acquired by a MBES through tilting and vertically oscillating the velocline. Figure 1 is an example of data which is believed to have been collected with the presence of internal waves in the watercolumn. The main objective of this work is to create a mathematical model to predict the uncertainty which is introduced into MBES soundings when internal waves are not accounted for in conventional ray tracing models. A secondary objective is to investigate the potential benefit of manipulating MBES water column imaging to account for the vertical oscillation of the velocline. Note that the uncertainty discussed in this paper is systematic because the uncertainty remains constant for any analysis of the same measurand, for this reason the uncertainty will be referred to as a bias throughout the paper.

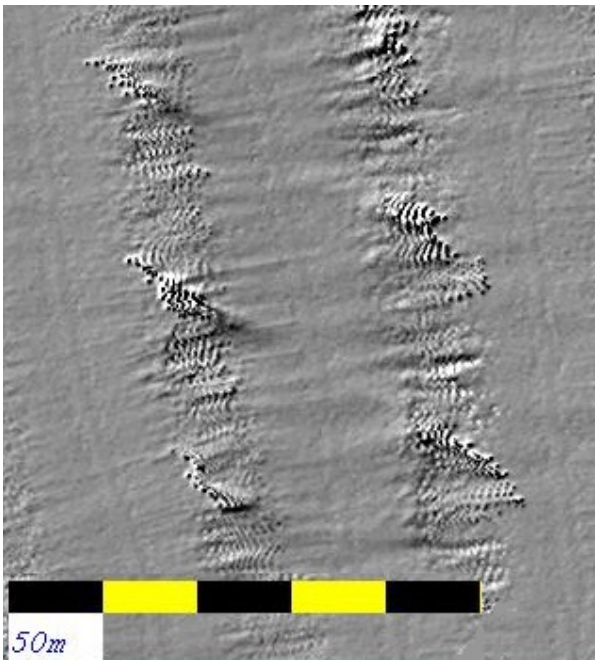

***Figure 1**: Gridded MBES data that is believed to have been collected with the presence of internal waves in the watercolumn. Data courtesy of Roger Flood.*

Internal waves and their effect on MBES soundings are discussed in section 2, followed by an outline of the fundamental calculations required to perform the simulation. Finally the model is used in a case study to demonstrate the general behaviour of the bias and

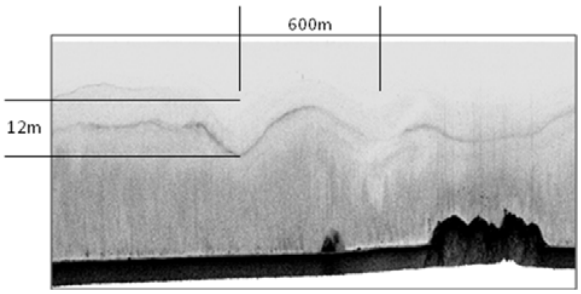

***Figure 2**: Along track vertical cross-section of water column scattering intensity showing the presence of an internal wave. (After Hughes Clarke 2006)*

2. Internal waves and their effect on MBES accuracy

An internal wave can be described as a gravity wave which propagates within the volume of any fluid. In the ocean, an internal wave is generated upon the disturbance of the pycnocline. The disturbance can be caused, for example, by flow near a shelf break or over a shoal. Once disturbed, the energy propagates away from the generation point as a wave that travels along the pycnocline (Apel 2004).

A large portion of observed internal waves fall into the category of internal solitary waves which are also referred to as solitons. Solitons occur as groups of oscillations that consist of up to a few dozen cycles. Solitons often have rank-ordered amplitudes and wavelengths, meaning the amplitude and wavelength are both largest on the leading wave and decay with each oscillation (Apel 2004). Typical values for continental shelf internal waves are listed in Table 1.

The shape of a soliton is considered by some to be almost sinusoidal (Sandstrom and Oakey 1994); however they tend to take on a more triangular shape because the wave troughs move faster than the peaks, which cause the gradient to be steeper between the two. This situation is caused by the propagation speed increasing when the isopycnals are displaced downward and decreasing along its upward motion (Sandstrom and Oakey 1994). For the mathematical model discussed in this work the idea of an internal wave taking the shape of a sinusoidal wave is used to facilitate the numerical simulation.

As mentioned in the introduction, internal waves introduce uncertainty through two mechanisms. The first is the vertical oscillation of the velocline; Figure 3 helps to describe the situation. The vertical oscillation of the velocline causes its true depth (dashed line) to differ from its assumed depth (solid line) which was recorded with an SSP. The depth discrepancy causes two effects. The first causes the calculated ray path (red line) to refract at a depth that is different than the true ray path (green line), which alters the ray's path. The second effect causes the two rays (true and calculated) to spend different amounts of time in each layer of sound speed. The overall distance a ray travels is a function of time and sound speed, so the second effect causes the overall length of each ray to be different.

***Table 1**: Typical characteristics of solitons. Adapted from (Apel 2004).*

Characteristic	Symbol	Scale
Packet Length	L (km)	1 – 10
Wave Height	$2\eta_0$ (m)	~15
Upper Layer Thickness	h_1 (m)	20 – 35
Lower Layer Thickness	h_2 (m)	30 – 200
Long Wave Speed	C0 (m/s)	0.5 – 1.0
Maximum Wavelength	λ_{max} (m)	100 – 1000
Crest Length	C_L (km)	0 - 30

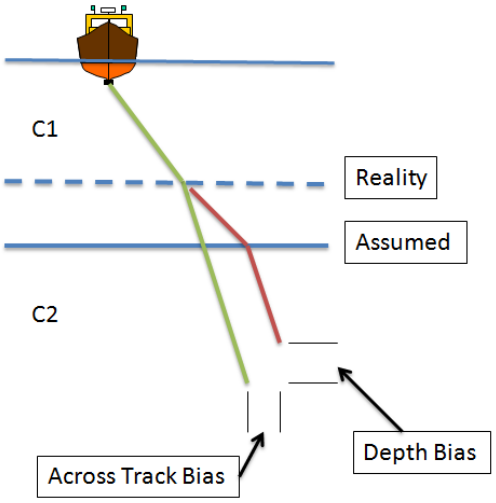

***Figure 3**: Effect of the velocline's vertical oscillation on MBES soundings*

The second mechanism through which internal waves introduce uncertainty into MBES soundings is tilting the velocline. The tilt violates the assumption that all layers of sound speed are horizontally stratified. Every degree of velocline tilt causes one degree of bias in the angle of incidence (Figure 4 (a)). Through Snell's law the incorrect incidence angle causes the refracted angle to be incorrect. It is an angular uncertainty that will cause both an across track (position) and depth uncertainty.

The problem is made even more complex by the fact that the internal wave causes the velocline to tilt about both the along track and across track axis. In the presence of a 2-axis tilt, the ray will no longer be constrained to a 2D plane (green plane in Figure 4 (b)). By ignoring the 3D aspect of the ray path, a bias results in the direction normal to the plane as this component can only be zero in a 2D ray tracing model. Uncertainty is also introduced into the depth and radial components of the ray traced solution as these components absorb the bias resulting from the 2D model's inability to account for the additional travel time associated with refracting out of the plane. One of the goals of this work is to gain an appreciation of the magnitude of the resulting bias; another goal is to gain a better understanding of the conditions under which this effect results in appreciable sounding bias.

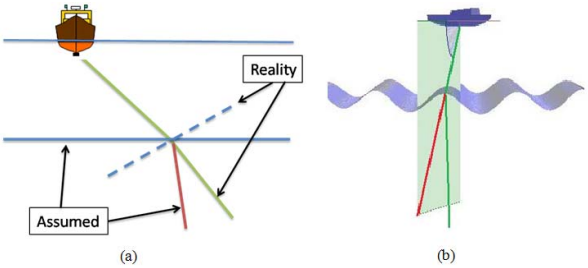

***Figure 4:** **(a)** Effect of across track tilt on refraction. **(b)** Effect of ignoring 3D refraction.*

3. Methods

Software was developed to simulate an estimate of the uncertainty introduced into MBES soundings by internal waves. The simulation requires several inputs to describe the characteristics of the watercolumn. The parameters are:

- the bearing of the survey lines relative to the direction that the internal wave propagates;
- water depth;
- sound speed above and below the velocline;
- the mean depth of the velocline;
- and finally the amplitude and wave length of the internal wave.

The software is currently designed to use equiangular 1° beam spacing with a 130° swath in an attempt to give a typical description of the uncertainty.
The foundation behind the software is that it traces the beam's path in 3D space instead of using the assumption that a beam is constrained by a 2D plane. The coordinate system used for the calculations is a right handed system. The x-axis is aligned with the direction of the internal wave's propagation, the z-axis is pointing down, the y-axis is oriented as to complete the right handed system, the internal wave is infinitely wide along the y-axis, and the origin is at the vessel's position during the first ping. This will be referred to as the internal wave coordinate system (IWCS, shown in Figure 5). The IWCS allows the vector representing the ships track relative to the internal wave to be calculated, simplifying the sounding coordinates by originally calculating them in the IWCS, rather than converting from ship based coordinates.

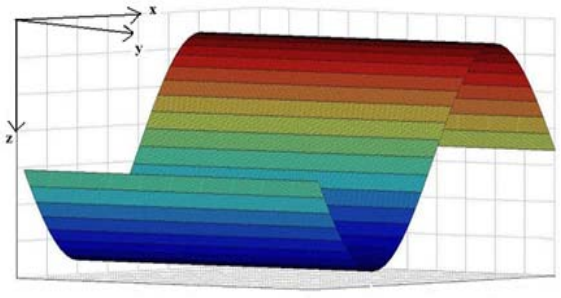

Figure 5: *Internal Wave Coordinate System.*

The simulation numerically models the path of an acoustic ray that travels through a water column which contains an internal wave and experiences three dimensional refraction based on the angle of incidence with the velocline and the sound speed in each layer (of a two layer water mass). Once it passes through the velocline the beam travels through the remainder of the water column until it strikes a synthetic flat seafloor at a user specified depth. The x, y, and z coordinates where the beam strikes the seafloor are used as the "true" coordinates (or solution) for the sounding; these are later compared with the biased solution for the same sounding..

Using the three dimensional Euclidean distance of the two line segments (above and below the velocline) and the corresponding sound speeds in each layer, the two-way travel time (TWTT) is calculated for the synthetic beam. The TWTT is meant to simulate the true time of flight that would have been measured under the specified circumstances. The synthetic TWTT is then used in a traditional 2D ray trace in order to get the coordinate solutions which have been biased by the internal wave (Figure 6). Each biased sounding is plotted onto a surface which represents the difference between the synthetic flat seafloor, and how the flat seafloor would appear if it were imaged through the specified internal wave. The above process repeats for each beam across the swath. The software simulates the vessel traveling over three cycles of the internal wave with sufficient pings in order for the difference surface to show how the pattern of the bias will develop.

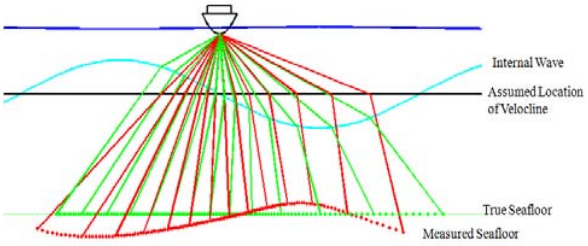

Figure 6 **:** *True ray paths vs. traditional ray trace.*

The same process is done with an augmented ray trace to evaluate the potential benefit of accounting for the velocline's true depth (*Figure 7*). In order to become augmented, the traditional ray trace is able to account for the true vertical position of the velocline across the entire swath (but does not attempt to account for potential tilting in either the across-track or along-track direction). This is done with the assumption that the depth of the velocline can be successfully imaged across the entire swath allowing for an adjustment in the SSP to replicate the correct depth of the velocline for every receiver beam. The first step in performing the augmented ray trace for a beam is to retrieve the z-coordinate (in IWCS) of the beam's intersection with the internal wave, which is calculated in the simulation. This value replaces the assumed depth of a horizontally stratified velocline (from the SSP). After the value is replaced, a traditional ray trace is performed, producing a sounding which only contains a bias from the tilting velocline and is free from any contamination by the velocline's varying depth.

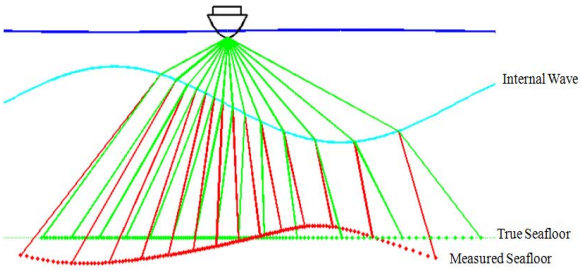

***Figure 7**: True ray paths vs. augmented ray trace.*

a) Three Dimensional Refraction

A velocline that is tilted in the along-track direction can cause a beam to deviate from the 2D plane by which it is assumed to be constrained. It is for this reason that the refraction of each beam must be calculated in 3D space, this requires the definition of the plane that contains: (1) a vector representing the ray direction in the upper layer, (2) the normal to the velocline at the point where the unit ray vector intersects the internal wave, and (3) a vector representing the direction of the refracted ray in the lower layer. The plane defined by these three vectors is referred to as the 3D refraction plane, note that it only differs from the 2D refraction plane by a rotation about the unit ray vector in the upper layer. Snell's law is applied to find the angle of refraction within this plane.
A unit vector representing the refracted ray in the lower layer is easily calculated in a coordinate system whose x-z plane is defined as the 3D refraction plane. A final transformation is thus required to bring the vector back into the IWCS. The following steps must be taken to achieve these results.

The first step in the process is calculating the IWCS coordinates for the point at which the ray intersects the internal wave. This is achieved by setting the x and z values from the unit vector representing the ray direction in the upper layer (B_1) equal to those from the surface representing the internal wave (IW) and solving for U. Equation (2) defines B_1, where δ is the ray's depression, β is the vessel's azimuth in the IWCS, and U is the scalar multiple which represents the length of the ray. Equation (3) defines IW, where d_i is the average depth of the internal wave, A is the internal wave's amplitude, ω is the angular frequency, and x is the x- coordinate in IWCS:

$$B_1 = U * \begin{bmatrix} -\cos\delta * \sin\beta \\ \cos\delta * \cos\beta \\ \sin\delta \end{bmatrix} \quad (2)$$

$$IW = d_i + A * \sin(\omega * x) \quad (3)$$

The line IW is stretched along the y-axis to create the surface. The result of the substitution is shown with equation (4):

$$B_1(z) * U = d_i + A * \sin[\omega * (x + B_1(x) * U)] \quad (4)$$

Equation (4) cannot be rearranged to solve for U so the equation is set equal to zero (equation (5)):

$$0 = di + A * \sin[\omega * (sonar(x) + Beam(x) * U)] - \text{Beam}(z) * U \quad (5)$$

and the bisection method is used to solve for the roots. Once the appropriate value for U is determined it is used in equation (2) to solve for the IWCS coordinates of the intersection point.
With the intersection coordinates calculated, the normal (N) to the velocline at that point is determined. This is done by taking the cross product of the two tangents to the velocline (tangent in the x direction, tangent in the y direction) at the point of intersection. The tangent in the y direction is always a unit vector running parallel to the y-axis because the surface is stretched along the y-axis, which also means the internal wave can be represented by a line in the x-z plane. The first step in calculating the tangent in the x direction is determining the slope of the line which is in the x-z plane. The slope at a specific value of x (equation (6)) is equal to the Δz which occurs when Δx is 1, allowing the tangent in the x direction to be represented using equation (7). The resulting vector is not of unit length however it is still in the correct direction and will not affect the calculations.

$$slope = A * \cos(\omega * x) * \omega \quad (6)$$

$$tangent\ x = \begin{bmatrix} 1 \\ 0 \\ slope \end{bmatrix} \quad (7)$$

The angle between the beam ($B1$) and the normal is calculated using the dot product in equation (8):

$$\theta_i = \cos^{-1}\left[\frac{N \cdot B1}{||N|| * ||B1||}\right] \quad (8)$$

where (θ_i) is the incidence angle. As explained, Snell's law is used to calculate the refracted angle (θ_r) within the 3D refraction plane. With this completed it is necessary to construct a new right handed coordinate system that has the incidence ray path as the x-axis, the normal to the refraction plane as the y-axis (calculated as the cross product of N and $B1$), and the z-axis defined by the cross product of the x and y axes.

$$B2 = \begin{bmatrix} \cos(\theta_i - \theta_r) \\ 0 \\ \sin(\theta_i - \theta_r) \end{bmatrix} \quad (9)$$

$$B2 = \begin{bmatrix} \cos(\theta_r - \theta_i) \\ 0 \\ -\sin(\theta_r - \theta_i) \end{bmatrix} \quad (10)$$

The final step is to rotate *B2* back into the IWCS, yielding a unit vector which represents the three dimensional direction of the refracted beam in the IWCS, *B3:*

$$B3 = inv(R) * B2 \quad (11)$$

The matrix *R* is the rotation matrix that is composed from the values which represent the axis of the new coordinate system within the IWCS. For example y_x is the y component of the new coordinate system's x axis defined in the internal wave system. The full matrix is represented by equation (12):

$$R = \begin{bmatrix} x_x & y_x & z_x \\ x_y & y_y & z_y \\ x_z & y_z & z_z \end{bmatrix} \quad (12)$$

Once B3 is calculated, the coordinates (in the IWCS) of its intersection with the plane representing the seafloor can be calculated, and are used as the "true" coordinates as previously explained in the Methods section.

b) Visualization of Results

Following the methodology outlined above, it is possible to calculate the 3D bias for a sounding that passes through an internal wave packet. Examination of the bias for all beam angles over the angular sector and over an entire internal wave packet is useful for examining how the bias evolves with beam angle and intersection point with the internal wave. A difference surface resulting from the biased 2D ray trace is useful for visualising the effect of the internal wave. Not surprisingly, an internal wave imprints a wave-like artifact on the synthetic flat seafloor (see Figure 8a). Figure 8b shows how the bias in depth varies as the vessel passes over an internal wave for the nadir ray and the outermost ray of the angular sector. Figure 8c shows the root mean square (RMS) of depth bias as a function of beam angle.

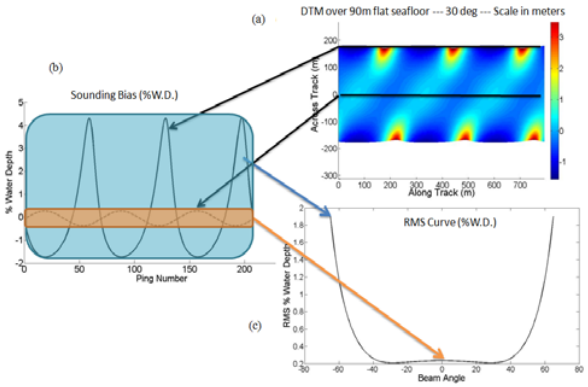

Figure 8: ***(a)*** *Surface representing the difference between the "true" flat seafloor, and the seafloor which has been biased by the internal wave.* ***(b)*** *Cross section of the sounding bias for all soundings by each beam (nadir & outer beam).* ***(c)*** *The depth RMS curve for figure 8 (a).*

The RMS curve is easy-to-understand and can be plotted with several other curves to compare how uncertainty changes with any of the parameters used in an analysis, e.g. amplitude of the internal wave, or depth of the velocline. The same process can be done for the horizontal position with the only difference being that the horizontal bias (Δh) for each sounding is calculated as $\Delta h = (\Delta x^2 + \Delta y^2)^{1/2}$.

4. Case Study

A two week research cruise was conducted by the Bedford Institute of Oceanography (BIO) in August of 1984 to study tidal processes in the Gully, a small canyon-like bathymetric feature located between Sable Island (to the west) and Banquereau Bank (to the east) on the Scotian Shelf (Sandstrom et al. 1988). Internal wave packets were imaged acoustically using a 200 kHz singlebeam echosounder (SBES) and were sampled with a towed undulating CTD. These data provide estimates of internal wave parameters that are useful as a case study in this work. Of particular interest is the internal wave packet observed during a four hour period on August 29th. The SBES water column reflectivity and the towed CTD measurements were able to record, among other things, the geometry of the internal waves as well as the sound speed information for the water column. The sound speed casts were retrieved from the World Ocean Database of 2005 (WOD05), and although it is not with 100% certainty that these casts were from the same project, the metadata indicates that they were taken on the exact date, time and location as the data discussed in Sandstrom et.al (1988). This means even if they are not from the same project they will at least provide similar sound speed values.

The plots and discussions from Sandstrom et al. (1988) provide all the necessary parameters to run through the simulation whereas the casts retrieved from WOD05 provide the speed of sound in the upper and lower layers. Table 2 lists the parameters used.

Parameter	Value
Wave Length	230m
Wave Height	32m
Depth of velocline	32m
Water Depth	90m
Sound speed above velocline	1485m/s
Sound speed below velocline	1459m/s

Table 2: *Banquereau Bank internal waves*

a) Digital Terrain Model

One of the goals of this research is to help identify when soundings have been collected through an internal wave so that hydrographers may be able to recognize the artifact. In order to achieve this goal the software has the ability to create a difference surface showing how the user-defined flat seafloor would appear if it were imaged through an internal wave as defined by the user parameters. This section presents those images with some qualitative analysis. The colour scales in the images represent the difference between each sounding's depth, and the depth of the flat seafloor.

Figures 9 and 10 (which are two different views of the same figure) are the result of using the Banquereau Bank internal wave parameters while traveling parallel to the direction that the wave propagates, i.e. the crests and troughs of the internal wave are perpendicular to the vessel course. The SSP cast is simulated to have identified the velocline at the average depth of the internal wave, which means the depth bias is equal and opposite at the tops and bottoms of the waves. Essentially it oscillates between the "smile" and "frown" that are synonymous with an incorrect depth of the velocline. In this situation, the depth uncertainty is dominated by the velocline's vertical oscillation. But as seen in figures 11 and 12 (which are two different views of the same figure), this changes as the direction of travel becomes oblique, and the depth uncertainty becomes dominated by tilting. Travelling at 30° relative to the wave's direction of propagation, the depth bias is much larger across the entire swath, reaching values over 3.5m. The oscillating smile and frown remain, but the smiles are much larger than the frowns (3.5m vs. 1.5m). The other interesting quality is how artifacts remain connected across the difference surface, and are aligned with neither the across track or along track axis. Rather they are aligned with the crest on the internal wave and are created by a series of pings. This unique quality presents itself as a good method for a hydrographer to identify the source of the artefact.

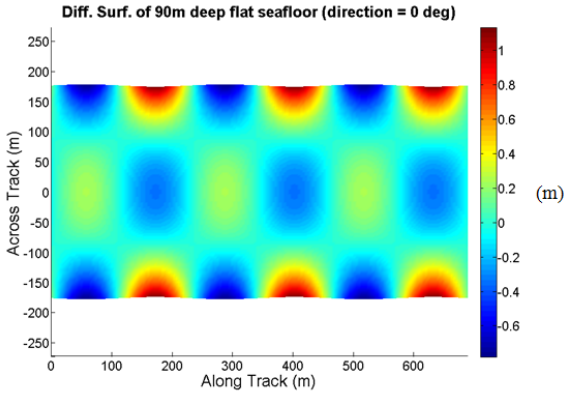

Figure 9: *Difference surface of 90m deep flat seafloor (direction = 0°).*

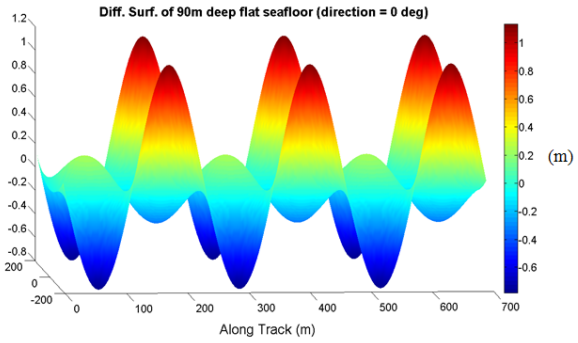

Figure 10: *Difference surface of 90m deep flat seafloor (direction = 0°).*

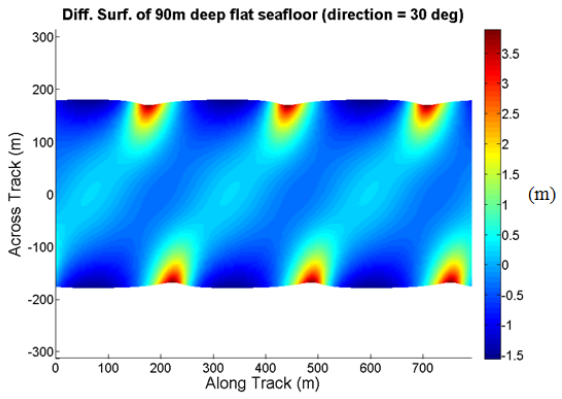

Figure 11: *Difference surface of 90m deep flat seafloor (direction = 30°).*

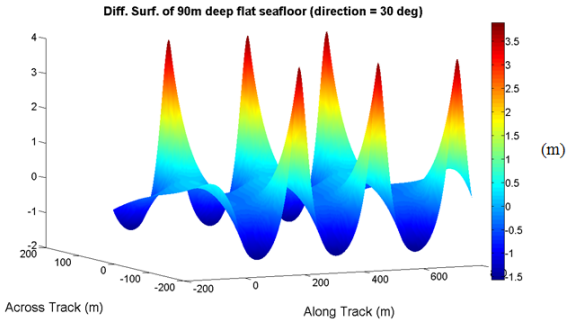

Figure 12: *Difference surface of 90m deep flat seafloor (direction = 30°).*

b) Direction of Travel

In this section the effect of changing the direction of travel relative to the internal wave's direction of propagation will be examined. Figures 13 and 14 are plots of the RMS curves where each colour represents a direction relative to the wave's propagation; the angles in degrees are listed in the legend. The plot for depth RMS also includes the allowable vertical uncertainty reduced to 1-sigma (divide by 1.96) according to the *Internal Hydrographic Organization's standards for hydrographic surveys* (IHO 2008). The allowable uncertainty is taken from Order 1A/1B because they would most likely be the standard used in the 90m water depth of the study area.

It is interesting to note in Figure 13 that the RMS curves for all the directions follow the same general trend. The RMS begins at approximately 0.15% of the water depth (%w.d.) at nadir and grows with the swath angle. Once the direction of travel moves beyond 0° a large portion of the swath (beams past +/- ~40°) has an RMS greater than the allowable uncertainty in 90m of water. The plot also shows that as the direction moves away from being parallel to the wave's propagation, the RMS grows at a greater rate with swath angle. These results mean that if it is possible to plan survey lines to run in the same direction that an internal wave propagates the uncertainty will be minimized (though it is fully realized that this may not always be practical or possible).

There are two important factors to keep in mind when looking at figures 13 and 14. The first is that they represent only the uncertainty created by the internal wave; once all other uncertainties for MBES systems are included the curves will be pushed up, resulting in a reduced usable swath width. The second is how RMS suppresses the maximum uncertainties. While traveling at 75°, the RMS reaches its highest values as it nears 3% w.d. in its outer beams. In this case the bias in the outer beams reaches values which near 12% w.d. (approximately 11m in 90m of water). When travelling at oblique angles over internal waves large discrepancies in the data should be expected.

The horizontal position RMS curves for the range of directions are plotted in Figure 14. The RMS remains relatively the same for all directions, and is within the allowable IHO order 1 A/B horizontal uncertainty of 3.87m (1-sigma). Note that 3.87m is the result of dividing the allowable total horizontal uncertainty (THU), which is expressed in the IHO standard at 95% confidence, by the 2D scaling constant specified in the IHO standard of 2.45 (IHO 2008). It appears as though the horizontal positions are within acceptable limits, however they are being compared to the minimum standards set out by the International Hydrographic Organization, which are meant to be used in the absence of any other guidance and are primarily designed for the production of navigational charts (IHO 2008). It is commonplace for more stringent standards to be set out in a contract, and it is likely that the standards would be considerably higher than the uncertainty introduced in the horizontal positions by internal waves (approx. 8% w.d. for the worst case scenario and 2% w.d. for the RMS of the outer beams).

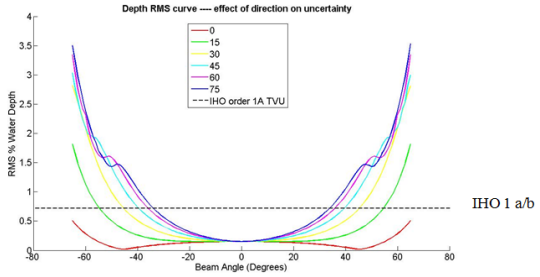

Figure 13: *Depth RMS for different directions at standard*

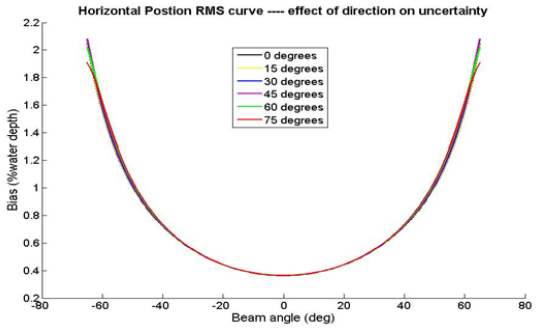

Figure 14: *Horizontal positions RMS for different directions.*

c) Augmented Ray Trace

As explained earlier, the simulator developed in this work has the ability to remove the uncertainty due to the vertical oscillation of the velocline.

The reason for doing this is to assess the potential benefit of adjusting the SSP to account for the varying depth of the velocline for every receiver beam by exploiting water column imaging. This section examines how the simulated Banquereau Bank soundings would improve with such an augmentation.

Both figures 15 and 16 contrast the RMS curves using a traditional 2D ray trace and an augmented 2D ray trace. Figure 15 is travelling parallel to the wave's propagation, whereas Figure 16 is at 30° to the direction of propagation. While travelling parallel to the internal wave propagation the uncertainty is nearly reduced to zero, being less than 0.05% of water depth at the outer beams; this small residual uncertainty is presumably due to the effects of along-track tilting. However while travelling at 30° there is only improvement in the nadir region.

By taking into account the depth of the velocline within the ray trace, the uncertainty for the vertical motion of the velocline is removed, leaving only the portion created by the tilting of the velocline. Through this logic it can be deduced that environments which have a larger fraction of the bias being created by the velocline's vertical displacement stand to have a larger percentage of their bias removed. Considering the previous statement, in terms of the results from the augmented ray trace, this means that while travelling parallel to the direction of propagation, the uncertainty is dominated by the velocline's vertical motion (there is only tilt in the along track direction), and at 30° it is dominated by the tilting (there is tilt in the along-track and across-track directions). For this case it can be concluded that the potential benefit from the augmented ray trace is only significant while travelling parallel to the internal wave's propagation.

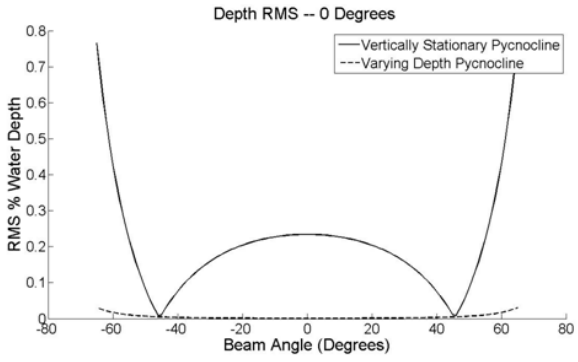

Figure 15: *Depth RMS improvement by tracking velocline depth (0°).*

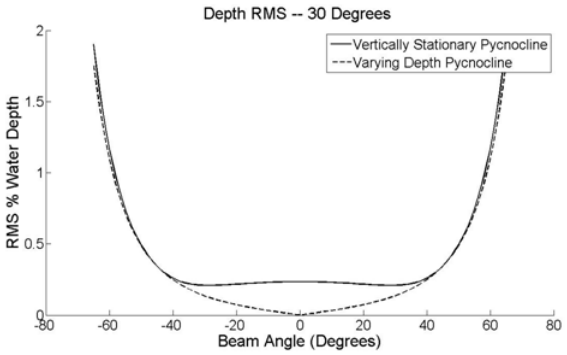

Figure 16: *Depth RMS improvement by tracking velocline depth (30°).*

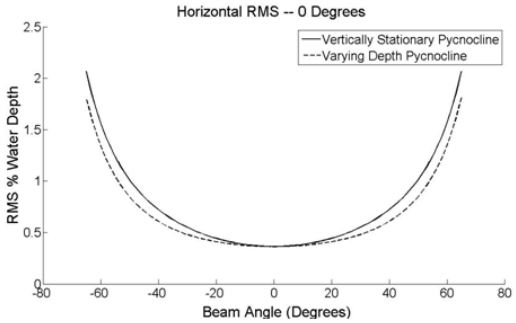

Figure 17: *Horizontal position RMS improvements by tracking velocline depth.*

Figure 17 shows that there is very little improvement in terms of the horizontal position from using the augmented ray trace. Also, unlike the depth bias, the improvement to the horizontal positions from using the augmented ray trace does not depend significantly on the direction of survey lines relative to internal wave propagation.

d) Sampling the Water Column

The case study has shown that failing to adequately model the effects of an internal wave on ray path propagation can lead to significant biases in MBES soundings. It has also shown that water column imaging methods have limited applicability (though improvements can be made to the augmentation that was applied, e.g. allowing for estimation of the across-track tilt of the velocline on a beam-by-beam basis). Can the problem be addressed instead through increased sound speed profiling?

Sampling equipment does exist that would allow for an increased ability to sample the water column, e.g. ODIM Brooke Ocean Moving Vessel Profiler (MVP) (Furlong et al. 1997).

Internal waves, however, present a unique challenge as the spatial distances over which the water column structure varies can be small compared to what can be realistically sampled using underway sound speed profiling equipment. An MVP's profiling rate (i.e. the maximum number of profiles that can be acquired over a defined time interval) is limited by the winch retrieval speed and maximum desired sampling depth. A downcast of a few tens of metres may take only seconds to complete, but the retrieval may take a few minutes resulting in large distances between samples. For example, a 3 minute profiling interval while travelling at 8 knots would yield a sound speed profile every 740 m. This is quite large when compared with the spatial wavelength of the internal waves observed over Banquereau Bank during the 1984 sampling campaign (~230 m). In this case, an extreme case of aliasing occurs when trying to sample the structure of the internal wave. The above situation is apparent in Figure 18 where the internal wave is plotted in green, roughly to scale for the above situation.

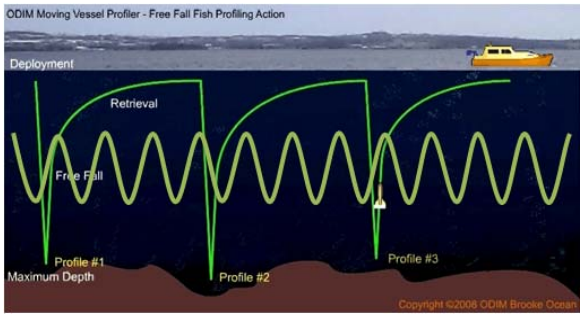

Figure 18: *Sound speed profiles using a MVP over an internal wave.*

Regardless of whether or not there is aliasing, the fact remains that using an SSP requires the assumption that the watercolumn is horizontally stratified. Even if it were possible to have a dense sampling over the internal wave, it would not account for the velocline's tilt, and won't represent the true velocline depth across the entire swath. This should not be misconstrued as saying that there is no advantage to densely sampling the water column. It is only meant to show that in areas with internal waves a hydrographer cannot expect to easily model the oceanographic conditions using sound speed profiles, even with hardware that allows for near continuous sampling of the water column.

5. Conclusions

Under certain conditions, internal waves in the water column can cause the total propagated depth uncertainty of MBES soundings to exceed IHO Order 1A/B specifications for a large portion of a typical MBES angular sector. It has been shown that planning survey lines to run parallel to the direction in which the internal waves propagate significantly reduces their effect. It has also been shown that augmenting traditional 2D ray tracing algorithms with water column imaging has the potential to minimize the uncertainty, however this approach is also limited to the case where survey line direction is parallel to the direction of internal wave propagation. Increasing sound speed acquisition rates can help only in cases where instrumentation can sample often enough to fully capture the nature of the wave.

Without a reliable method for reducing the impact of internal waves on sounding accuracy, perhaps the best approach to dealing with internal waves is a background study of the oceanographic processes at work in the area to be surveyed. With information about the geometry of internal waves, the numerical simulation outlined in this work has potential to assist in creating a more accurate assessment of the expected total propagated uncertainty at the survey design stage. This might allow the hydrographer to estimate parameters such as survey line direction and spacing better. Furthermore, oceanographic background research could also be used to identify periods characterized by low internal wave activity. These "windows of opportunity" would allow the surveyor to work around the problem and avoid high costs associated with reduced line spacing when working in the worst of conditions.

6. Future Work.

The uncertainty discussed in this paper is a systematic uncertainty, meaning that if the true geometry of any specific wave can be identified, the 3D refraction algorithm outlined in this work can be used to correct any erroneous data. The key to this is being able to measure the true geometry of the wave. The potential future of this research is to investigate the possibility of exploiting water column imagery by digitizing the visible impedance contrast caused by the sharp density gradient along the internal wave. The digitized surface should provide a correct depth and incidence angle for each receiver beam ray path. If successful it would provide a method of correcting the artifacts from any phenomena that result in significant tilting or oscillation of the velocline in post processing; however its utility will hinge on willingness to continuously collect water column data.

It should be noted that the results of this work are preliminary. Further research and testing will:

- verify the fidelity of the numerical simulation through field trials
- assess the feasibility and practicality of identifying internal wave propagation direction (if there is only one) and adjusting the direction of survey lines to run parallel to the internal wave propagation

- explore the dependability of multibeam water column imaging to produce images of internal waves which are distinguishable from the surrounding noise in the water column.

References

- Apel, J.R. (2004). Oceanic Internal Waves and Solitons. In *An Atlas of Oceanic Internal Solitary Waves*, Global Ocean Associates, Alexandria, Virginia. 1-40.
- Baum, S.K. (2004). *Glossary of Physical Oceanography and Related Disciplines*. Department of Oceanography, Texas A&M University.
- Furlong, A., Beanlands, B., and Chin-Yee, M. (1997). Moving vessel profiler (MVP) real time near vertical data profiles at 12 knots. In Proc. of Oceans '97 Conference, Halifax, Canada.
- Hughes Clarke, J. (2006). Applications of multibeam water column imaging for hydrographic survey. *The Hydrographic Journal.* April issue.
- International Hydrographic Organization (2008). IHO Standards for Hydrographic Surveys. Special Publication No. 44 5th Edition, Monaco.
- Lurton, X. (2002). *An Introduction to Underwater Acoustics: Principles and Applications*. Praxis Publishing Ltd., United Kingdom.
- Sandstrom, H., J.A. Elliott, and N.A. Cochrane (1988). Observing Groups of Solitary Internal Waves and Turbulence with BATFISH and Echo-Sounder. *Journal of Physical Oceanography,* 19, 987-997.
- Sandstrom, H., and N.S. Oakey (1994). Dissipation in Internal Tides and Solitary Waves. *Journal of Physical Oceanography,* 25, 604-614.

Biographies of the authors

Travis Hamilton has his Bachelor's degree in Geodesy and Geomatics Engineering (2010) from the University of New Brunswick. He was first attracted to the field of hydrographic surveying after being offered an opportunity to work in the Arctic with the Ocean Mapping Group at UNB in 2009.
Currently Travis is working on his Msc in Geodesy and Geomatics Engineering at UNB. The focus of his Msc research is in the estimation of sounding uncertainty from non-horizontal refracting layers.

Jonathan Beaudoin has a PhD (2010) in Geodesy and Geomatics Engineering from the University of New Brunswick and Bachelor's degrees in Geodesy and Geomatics Engineering (2002) and Computer Science (2002), also from UNB.
Having just arrived at CCOM in the Spring of 2010, he plans to carry on in the field of his PhD research, that of estimating sounding uncertainty from measurements of water mass variability. His research plans include an examination of oceanographic databases such as the World Ocean Atlas and the World Ocean Database to see how the data contained in these comprehensive collections can be turned into information that is meaningful to a hydrographic surveyor. Other plans involve assessing how to best acquire, visualize, process and analyse data from high-resolution underway sound speed sampling systems, again, in terms that are meaningful to a hydrographic surveyor.